JPET Fast Forward. Published on May 7, 2018 as DOI: 10.1124/jpet.118.249151
This article has not been copyedited and formatted. The final version may differ from this version.

Survivin inhibitors mitigate chemotherapeutic resistance in breast cancer cells by suppressing genotoxic NF-kappaB activation.

Wei Wang, Bo Zhang, Arul M. Mani, Zhongzhi Wu, Yu Fan, Wei Li, Zhao-Hui Wu

Department of Pathology and Laboratory Medicine, Center for Cancer Research (WW, BZ, ZHW), Department of Physiology (AMM), Department of Pharmaceutical Sciences (ZW, WL), University of Tennessee Health Science Center; Cancer Institute (YF), the Affiliated People's Hospital of Jiangsu University, China

JPET Fast Forward. Published on May 7, 2018 as DOI: 10.1124/jpet.118.249151
This article has not been copyedited and formatted. The final version may differ from this version.

Running title: Survivin inhibitors sensitize TNBC to chemotherapy

Corresponding Author: Zhao-Hui Wu, University of Tennessee Health Science Center, 19 South Manassas Street, Memphis, TN38163. Phone: 901-448-2612; Fax: 901-448-3910; Email: zwu6@uthsc.edu;

Co-corresponding author: Wei Li, University of Tennessee Health Science Center, 881 Madison Avenue, Memphis, TN 38163. Phone: 901-448-7532; Fax: 901-448-6828; E-mail: wli@uthsc.edu.

Number of text pages: 27

Number of tables: 0

Number of figures: 6

Number of references: 47

Number of words in the Abstract: 208

Number of words in the Introduction: 706

Number of words in the Discussion: 1200

Abbreviations: CI, combination index; CPC, chromosomal passenger complex; EMT, epithelial-mesenchymal transition; ER, estrogen receptor; HER2, epidermal growth factor receptor 2; IAP, Inhibitor-of-Apoptosis Proteins; IR, ionizing radiation; NEMO, NF-κB essential modulator; NF-κB, nuclear factor kappa B; NSG, NOD scid gamma; OS, overall survival; PR, progesterone receptor; RFS, relapse free survival; SMAC, second mitochondria-derived activator of caspases; STR, Short Tandem Repeat; TNBC, triple negative breast cancer

Recommended section assignment: Drug Discovery and Translational Medicine

JPET Fast Forward. Published on May 7, 2018 as DOI: 10.1124/jpet.118.249151
This article has not been copyedited and formatted. The final version may differ from this version.

Abstract

Therapeutic resistance developed after chemotherapy and aggressive metastasis are the major causes for cancer-related death in triple negative breast cancer (TNBC) patients. Survivin is the smallest member of Inhibitor-of-Apoptosis Proteins (IAPs) family, which plays critical roles in cell division and cell survival. High expression levels of survivin have been associated with therapeutic resistance in various cancers. We recently developed a novel small molecule survivin inhibitor mimicking IAP-binding motif of second mitochondria-derived activator of caspase, which showed high potency in promoting survivin degradation. Here, we show survivin inhibitors MX106/MX107 suppress TNBC cell proliferation. Moreover, MX106/MX107 synergized with chemotherapeutic drugs or radiation, and significantly enhanced tumoricidal efficacy of genotoxic treatments. Mechanistically, MX106/MX107 induced degradation of XIAP and/or cIAP1, which inhibited NF-κB activation by genotoxic agents. Treatment with MX106/MX107 alone did not activate alternative NF-κB signaling in breast cancer cells, which likely is owing to their selective potency in degrading survivin in these cells. Additionally, survivin degradation by MX106/MX107 dramatically increased abnormal mitotic spindle formation and cell division failure, which led to cell cycle arrest in breast cancer cells. Overall, our study suggests that combination treatment of TNBC using survivin inhibitors MX106/MX107 with cytotoxic chemotherapeutic drugs can achieve significantly improved therapeutic efficacy, which depends on MX106/MX107-mediated inhibition of genotoxic NF-κB activation.

JPET Fast Forward. Published on May 7, 2018 as DOI: 10.1124/jpet.118.249151
This article has not been copyedited and formatted. The final version may differ from this version.

Introduction

Triple negative breast cancer (TNBC) is a heterogenic breast cancer subtype which lacks hormone receptors (ER/PR) and human epidermal growth factor receptor 2 (HER2). In the absence of approved molecular targeted therapy, cytotoxic chemotherapy remains as the standard of care for treating TNBC patients (Bianchini et al., 2016). Although most TNBC patients respond to chemotherapy initially, many of them develop drug resistance and suffer rapid relapse within 2-3 years following the initial treatment. Moreover, TNBC is characterized by aggressive invasion and unique pattern of metastases, which may further contribute to the rapidly arising resistance developed in TNBC patients (Foulkes et al., 2010). More effective treatments and novel approaches to mitigate drug resistance are in urgent need for improving the clinical outcome of TNBC patients.

A variety of molecular mechanisms have been demonstrated to promote therapeutic resistance, among which transcription factor NF-κB was found to play critical roles in mediating both intrinsic and acquired therapeutic resistance in cancer cells (Nakanishi and Toi, 2005; Baldwin, 2012; Holohan et al., 2013). Activation of NF-κB promotes cell proliferation, inhibits apoptosis and drives inflammatory microenvironment, which all could contribute to cancer progression and therapeutic resistance. Additionally, crosstalk between NF-κB with the other signaling cascades including JAK/STATs, Wnt/β-catenin and TGFβ pathways further facilitates the development of drug resistance by promoting epithelial-mesenchymal transition (EMT) and self-renewal of tumor initiating cell/cancer stem-like cell population (Singh and Settleman, 2010; Mitra et al., 2015; Zheng, 2017). Our previously studies revealed a retrograde nuclear-to-cytoplasmic signaling cascade which mediates DNA damaging agent-induced NF-κB activation (Wu and Miyamoto, 2007; McCool and Miyamoto, 2012). In this genotoxic NF-κB signaling pathway, NEMO (NF-κB essential modulator, also known as IKKγ) functions as the messenger to relay nuclear DNA damage signal into cytoplasmic NF-κB/IKK machinery through its

JPET Fast Forward. Published on May 7, 2018 as DOI: 10.1124/jpet.118.249151
This article has not been copyedited and formatted. The final version may differ from this version.

sequential modification such as sumoylation, phosphorylation and ubiquitylation (Huang et al., 2003; Wu et al., 2006; Wu et al., 2010). Moreover, we and other labs also identified a number of critical regulators, such as ATM, PIASy, cIAP1, PARP1, TRAF6, XIAP1, ELKS and SAM68, which play essential roles in modulating this genotoxic NF-κB signaling pathway (Mabb et al., 2006; Jin et al., 2009; Stilmann et al., 2009; Hinz et al., 2010; Wu et al., 2010; Fu et al., 2016). In response to chemotherapeutic treatments or radiation, this atypical NF-κB signaling cascade is activated in cancer cells, which enhances the transcription of a variety of protein-coding genes and miRNAs, promoting drug resistance and invasiveness of cancer cells (McCool and Miyamoto, 2012; Niu et al., 2012; Niu et al., 2013; Niu et al., 2016).

Survivin (BIRC5) is the smallest member of the inhibitor-of-Apoptosis proteins (IAPs) family, which also includes cIAP1/2 and XIAP. Survivin expression is frequently increased in various cancers and has been associated with chemoresistance and poor prognosis in cancer patients (Altieri, 2015; Peery et al., 2017). The oncogenic roles of survivin mainly depend on its function in inhibiting apoptosis and as a key mitotic regulator (Altieri, 2015; Garg et al., 2016). In normal cells, survivin expression is abundant during embryonic and fetal development stages. In contrast, survivin level becomes almost undetectable in terminally differentiated adult cells (Altieri, 2015). Therefore, the increased expression of survivin in most cancer cells makes it an attractive cancer-specific target for cancer treatment. We recently developed and optimized a potent small molecule inhibitor of survivin based on a tetrapeptide motif (AVPI) harbored in the endogenous IAP antagonist, second mitochondria-derived activator of caspases (SMAC) (Wang and Li, 2014; Xiao and Li, 2015; Xiao et al., 2015). We found this small molecule inhibitor UC-112 and its derivatives MX106/MX107 efficiently induced proteasome-dependent degradation of survivin in a number of cancer cell lines. In addition to survivin, these small molecules also promotes degradation of other IAPs, such as cIAP1/2 and XIAP, with reduced potency and in a cell type-dependent manner. Moreover, we showed that our survivin inhibitors significantly

reduced melanoma cells growth *in vitro* and in xenograft mouse model, suggesting their potential anti-melanoma efficacy (Wang and Li, 2014; Xiao et al., 2015).

Here we show that survivin inhibitors MX106/MX107 suppress TNBC cell growth *in vitro* and in an orthotopic xenograft model. Moreover, MX106 showed robust synergism with chemotherapeutics and ionizing radiation (IR) in inhibiting proliferation and promoting apoptosis in cancer cells. Mechanistically, MX106/MX107 suppressed DNA damage-induced NF-κB activation which depends on degradation of cIAP1 and XIAP. In contrast, survivin is not required for genotoxic NF-κB activation whereas its depletion leads to cell cycle arrest and mitotic catastrophe in TNBC cells. We further found that combination treatment of survivin inhibitor with doxorubicin efficiently reduced TNBC xenograft tumor growth with significantly increased tumor-suppressive efficacy compared with either drug alone. Our results suggest that small molecule survivin inhibitor may also be used for treating TNBC, especially in combination with cytotoxic chemotherapeutics. This combinatory regimen remarkably reduced drug resistance developed in TNBC cells by inhibiting NF-κB, which sensitized TNBC cells to lower dose of doxorubicin treatment with improved efficacy.

Materials and Methods

Cells, plasmids and regents

HEK293T cells, human breast cancer cell line MDA-MB-231 cells and human bone osteosarcoma cell line U2OS cells were obtained from ATCC and cultured in DMEM supplemented with 10% fetal bovine serum. Both MDA-MB-231 and U2OS cells were derived from females. Cells resuscitated from original passage and passaged within 6 months were used in all experiments. ATCC cell lines were characterized by Short Tandem Repeat (STR) profiling. The Myc-NEMO plasmid was generated by cloning the human NEMO coding sequence into the pcDNA3 vector as reported previously (Wu et al., 2006). Compounds MX106

JPET Fast Forward. Published on May 7, 2018 as DOI: 10.1124/jpet.118.249151
This article has not been copyedited and formatted. The final version may differ from this version.

(previously denoted as 4g) and MX107(previously denoted as 4f) were synthesized and characterized as previously reported (Xiao et al., 2015). Etoposide (VP16) and Doxorubicin (Dox) were purchased from Sigma-Aldrich.

Combination index (CI) calculation

The effect of the combination of Dox with MX106 was determined by CompuSyn program (ComboSyn). Drug concentrations were designed based on the IC_{50} value of each drug tested. Synergism, additive activity or antagonism was determined by the Chou-Talalay method (Chou, 2010) and calculated with a CI using the CompuSyn.

Immunofluorescence

Cells were seeded on glass coverslips and treated by MX106 or DMSO for 24h. Then, treated cells were fixed with 4% paraformaldehyde for 15 minutes, followed by permeabilization with 0.2% Triton X-100 for 5 minutes, cells then were blocked with 3% bovine serum albumin for 15 minutes, incubated with the primary antibody (α-Tubulin) for 1 hour, and incubated with fluorescence-conjugated secondary antibody for 1 hour. Finally, cells were imaged with a fluorescent microscope (Invitrogen). Nuclei were visualized by DAPI staining.

Immunoprecipitation and detection of ubiquitylation

Briefly, cells were lysed with 1% SDS in IP lysis buffer (20 mm Tris (pH 7.0), 250 mm NaCl, 3 mm EDTA, 3 mm EGTA, 0.5% Nonidet P-40, 2 mm DTT, 0.5 mm PMSF, 20 mm β-glycerol phosphate, 1 mm sodium orthovanadate, 1 μg/ml leupeptin, 1 μg/ml aprotinin, 10 mm p-nitrophenyl phosphate, and 10 mm sodium fluoride) at 95 °C for 30 min. The cell lysates were then diluted with IP lysis buffer to reduce SDS to 0.1% and mixed with primary antibodies and protein G-Sepharose for incubation at 4 °C overnight. The precipitated proteins were resolved on SDA-PAGE and the ubiquitylation of precipitated proteins was examined by immunoblotting.

***in vitro* kinase assay**

JPET Fast Forward. Published on May 7, 2018 as DOI: 10.1124/jpet.118.249151
This article has not been copyedited and formatted. The final version may differ from this version.

A total of 2×10^6 cells were treated as indicated. Cell pellets were lysed in 10% PBS and 90% IP lysis buffer (20 mM Tris [pH 7.0], 250 mM NaCl, 3 mM EDTA, 3 mM EGTA, 0.5% NP-40, 2 mM DTT, 0.5 mM PMSF, 20 mM β-glycerol phosphate, 1 mM sodium orthovanadate, 1 μg of leupeptin/ml, 1 μg of aprotinin/ml, 10 mM p-nitrophenyl phosphate, 10 mM sodium fluoride). Supernatants were diluted further in lysis buffer, and 1 μg of α-TAB2 antibody (TAK1 KA) or α-IKKγ antibody (IKK KA) was added to each tube. Protein G-Sepharose enriched IP samples were washed three times in lysis buffer and three times in TAK1 kinase buffer (50mM Tris-HCl, pH7.5, 0.5 mM DTT, 5 mM MgCl2, 50 μM ATP) or IKK kinase buffer (20 mM HEPES, pH 7.7, 2 mM MgCl2, 2 mM MnCl2, 1 mM DTT, 10 μM ATP) supplemented with the panel of inhibitors as above. The kinase activity was assayed in the respective kinase buffer with 1 μg of substrate (GST-IKKβ166–197 for TAK1 KA, and GST-IκBα1–56 for IKK KA) and 1 μCi of [γ-32P] ATP for 45 min at 30°C. The samples were boiled in 2xSDS loading buffer, separated by SDS-PAGE, and transferred to PVDF membranes. Radioactive signals were captured by Phosphoimage screen, and analyzed by ImageQuant software. The membranes were subjected to Western blotting.

In vivo xenograft model

Female NOD scid gamma (NSG) mice (age 6 wk) from Jackson Lab were maintained in the UTHSC animal facility. All animal studies were conducted in accordance with NIH animal use guidelines and approved by UTHSC IACUC. 1×10^6 MDA-MB-231 LM2 cells were injected into mice mammary fat pad (2/each mice). Tumor growth was monitored by caliper measurement using the formula ($width^2 \times length/2$) (mm^3). When tumor volume reached ~100 mm^3, tumor-bearing mice were randomly divided into 4 groups, and treated with intraperitoneal injection of PBS vehicle, Dox (1.5 mg/kg, once a week, every Monday), MX106 (20 mg/kg/day, 5d/week, Mon-Fri), or in combination of Dox and MX106 (same dosage and schedule as single treatment). AT the end point, the mice were sacrificed and primary tumors were isolated for

further analyses. Group assignment and tumor monitoring were carried out double-blinded. Mice were also imaged by Xenogen IVIS system (Perkin-Elmer) to visualize primary tumors and lung metastases.

Statistical Analysis

The results were presented as Mean ± SD, and analyzed with one-way ANOVA or Student's t-test. Disease free survival/overall survival analysis was estimated by the Kaplan-Meier method. All statistical analyses were performed using SPSS 22.0 software (SPSS Inc). $P<0.05$ was denoted as statistically significant.

Results

Survivin inhibitors sensitize cancer cells to genotoxic treatments

Increased survivin expression was found in various stages of breast cancer tissues compared to normal breast tissues (Ryan et al., 2005). Higher survivin levels also correlated with more advanced breast cancers and metastasis (Li et al., 2017). Using KM-Plotter (Lanczky et al., 2016), we determined the correlation between survivin expression levels with overall survival (OS) in 1402 breast cancer patients. High survivin level significantly associated with poor overall survival in breast cancer patients (HR=2.58, 95% CI: 1.94-3.44, p=1.9e-11; Fig. 1A, left). In the TNBC patients, higher survivin expression strongly correlated with shorter relapse free survival (RFS) in TNBC patients (HR=2.19, 95% CI: 1.34-3.59, p=0.0014; Fig. 1A, right). These data suggest that increased survivin plays critical roles in promoting breast cancer progression and relapse.

To determine whether survivin inhibitor decreases TNBC cell viability, we treated MDA-MB-231 cells with varying doses of MX106 or MX107 for 24 h. Both MX106 and MX107 effectively suppressed MDA-MB-231 cells proliferation with IC_{50} around 2-3 μM (Fig. 1B). Moreover,

JPET Fast Forward. Published on May 7, 2018 as DOI: 10.1124/jpet.118.249151
This article has not been copyedited and formatted. The final version may differ from this version.

combining MX106 with doxorubicin (Dox) significantly enhanced the tumoricidal efficacy of Dox in TNBC cells, compared with Dox treatment alone (Fig. 1C). The IC_{50} of Dox to MDA-MB-231 cells decreased from 31.95 ng/ml to 1.62 ng/ml, a drop of almost 20 folds, suggesting a synergistic effect between these two drugs. To validate this synergism, we determined the combination index (CI) value for combination of MX106 and Dox following the reported algorithm (Chou, 2010). We found CI of this two-drug combination in MDA-MB-231 cells is 0.016 at ED_{50} (Fig. 1D, supplemental Tab. 1), suggesting a strong synergistic effect between MX106 and Dox. Interestingly, although another survivin inhibitor YM155 showed higher potency in inhibiting MDA-MB-231 cells growth (IC50=3.7nM, supplemental Fig. 1A), MX106 showed substantially enhanced CI when combined with Dox compared with YM155, suggesting a robust synergism between MX106 and Dox in inhibiting MDA-MB-231 cells proliferation (supplemental Tab. 1, supplemental Fig. 1B). Additionally, combination treatment with MX106 also substantially enhanced the tumoricidal effect of Dox in osteosarcoma U2OS cells (Fig. 1E). Moreover, when we combined MX106 with IR for treating MDA-MB-231 cells, enhanced tumoricidal effect was also observed in combinatory treatment compared to IR alone (Fig. 1F). All these results strongly suggest that survivin inhibitors MX106/MX107 could synergize with genotoxic drugs and radiation, resulting in significantly improved anti-tumor efficacy of these cytotoxic treatments.

Survivin inhibitors enhance genotoxic treatment-induced apoptosis

We found combination treatment of MX106 and Dox substantially decreased MDA-MB-231 cell survival, compared with treatment with either MX106 or Dox (Fig. 2A). To determine whether survivin inhibitor enhances Dox-induced cancer cell apoptosis, we carried out flow cytometry analysis with PI/Annexin V staining in MDA-MB-231 cells treated by MX106, Dox or in combination. Interestingly, treatment with MX106 alone (2 μM) did not significantly increase apoptosis in MDA-MB-231 cells. In contrast, combination treatment of MX106 with Dox doubled

apoptotic population compared with that by Dox alone (Fig. 2B). Consistent with flow cytometry data, we also detected significantly increased PARP1 cleavage and Caspase3 activation in cells treated by chemodrug etoposide (VP16) or Dox in combination of either MX106 or MX107, compared to cells treated with Dox alone (Fig. 2C-D). Meanwhile, we did not observe strong activation of Caspase 3 and PARP-1 cleavage in cells treated by MX106 or MX107, suggesting that the tumor suppressive effect of MX106/MX107 on MDA-MB-231 cells we observed likely depends on proliferation inhibition.

MX106/MX107 diminishes genotoxic agent-induced NF-κB activation.

Our previous studies demonstrated that genotoxic agents, such as Dox and IR, could activate NF-κB, which inhibits genotoxic treatment-induced apoptosis in cancer cells (McCool and Miyamoto, 2012; Wang et al., 2017). We found co-treatment of MX106 with Dox substantially decreased Dox-induced NF-κB activation (Fig. 3A). This inhibition of genotoxic stress-induced NF-κB is not limited to MDA-MB-231 cells or Dox treatment, since we observed similar inhibition of NF-κB signaling in HEK293 cells treated with IR and U2OS cells exposed to Dox (Fig. 3B-C). In these cells, we noticed that along with dramatic decrease of survivin expression upon MX106/MX107 treatment, the expression of other IAPs, such as cIAP1 and XIAP, also decreased to varying extent depending on the cell type (Fig. 3A-C). XIAP and cIAP1 has been shown to be required for genotoxic NF-κB signaling in various cancer cells (Jin et al., 2009; Hinz et al., 2010; Wu et al., 2010). Consistently, we observed inhibition of NF-κB activation by pre-treatment of MX106/MX107 in HEK293 cells stimulated by VP16, which correlated with significantly decreased expression of cIAP1, XIAP and survivin (Fig. 3D). In contrast, YM155 treatment did not decrease cIAP1 and XIAP level in MDA-MB-231 cells although survivin was substantially suppressed (supplemental Fig. 1C). Meanwhile, Dox-induced NF-κB activation was not inhibited by YM155.

Previous reports showed that SMAC memetic such as BV6 and compound A (Varfolomeev et al., 2007; Vince et al., 2007), which both induce rapid cIAP1 degradation, activates alternative NF-κB signaling pathway. We found that treatment with MX106 up to 24h did not substantially increase p52 processing, which correlates with incomplete cIAP1 depletion in cells treated with MX106 (supplemental Fig. 2A). Neither did we observe obvious change of classical NF-κB activation by TNFα in cells treated with MX106 or MX107 (Fig. 3D). These data suggest that survivin inhibitor MX106/MX107 predominantly suppress genotoxic NF-κB signaling.

We further validate the impact of survivin inhibitors on genotoxic NF-κB activation by reporter assay. Accordingly, MX106/MX107 significantly inhibited the transactivity of NF-κB in MDA-MB-231 cells treated by Dox (Fig. 3E). Moreover, Dox-induced upregulation of canonical NF-κB-target genes, such as IκBα (*NFKBIA*), IL-6 (*IL6*) and IL-8 (*CXCL8*), was substantially suppressed by MX106/MX107 (Fig. 3F). All these data strongly support that survivin inhibitor MX106/MX107 could diminish genotoxic agent-induced NF-κB activation and suppress its downstream target gene transcription, which may play a role in enhancing cancer cell sensitivity to genotoxic treatments and promoting apoptosis.

MX106/MX107 interfere genotoxic NF-κB signaling by suppressing cIAP1/XIAP-mediated ubiquitylation.

We previously showed that NEMO mono-ubiquitylation is essential for NEMO export from nucleus and subsequent IKK activation in cytoplasm (Huang et al., 2003; Wu et al., 2006). Further studies showed that cIAP1 is an essential ubiquitin E3 ligase for mediating NEMO mono-ubiquitylation (McCool and Miyamoto, 2012; Holohan et al., 2013). Since our survivin inhibitors also decrease levels of cIAP1 in cells, we examined whether MX106/MX107 also affect NEMO mono-ubiquitylation upon genotoxic treatment. Indeed, NEMO mono-ubiquitylation was decreased in HEK293 cells treated by VP16 in combination with MX106 or MX107 (Fig.

4A). Consistently, we found VP16-induced K63-linked polyubiquitylation of ELKS, another key modulator of genotoxic NF-κB signaling (Wang et al., 2017), was also diminished by MX106/MX107 (Fig. 4B). This inhibition of ELKS K63-ubiquitylation is likely due to MX106/MX107-induced downregulation of XIAP, which is also required for ELKS ubiquitylation upon genotoxic stress.

Previous reports have shown that NEMO mono-ubiquitylation and ELKS K63-ubiquitiylation are essential for TAK1/IKK kinase cascade activation upon genotoxic treatments (Wu et al., 2006; McCool and Miyamoto, 2012; Wang et al., 2017). As shown in Fig 4C-D, we observed a dramatically decreased activation of TAK1 and IKK by VP16 in cells co-treated with MX106 or MX107 using *in vitro* kinase assays. Altogether, these results indicate that the survivin inhibitor MX106/MX107 could suppress DNA-damage-induced NF-κB kinase cascade activation by attenuating essential upstream ubiquitylation events.

Survivin is dispensable for genotoxic NF-κB activation, but is essential for cell cycle progression in cancer cells.

Since it is unclear whether survivin plays a role in mediating NF-κB activation by genotoxic treatment, we knocked down survivin with specific siRNA in HEK293 cells and examined NF-κB activation by genotoxic drug VP16. Depletion of survivin has little effect on VP16-induced NF-κB activation (Fig. 5A). Similar results were also observed in MDA-MB-231 cells treated with Dox (data not shown). These observations indicate survivin is not required for effective NF-κB activation by genotoxic treatments.

Survivin is a member of the chromosomal passenger complex (CPC) along with Aurora B, Borealin and INCEP, which play essential role in regulating chromosome-microtubule attachment, spindle assembly checkpoint, and cytokinesis during mitosis and cell division (Carmena et al., 2012). Depletion of survivin has been shown to lead to abnormal cell division

and mitotic catastrophe (Altieri, 2015). We treated MDA-MB-231 cells with MX106 for 48 hours. In accordance of previous reports (Pennati et al., 2004; Kedinger et al., 2013), depletion of survivin led to cell cycle arrest at G2/M phase (Fig. 5B). Moreover, aberrant mitotic progression indicated by increased fraction of polyploid cells with more than 4N DNA content was observed in MDA-MB-231 cells treated by MX106. This observation is consistent with the essential role of survivin in proper completion of mitosis and cell division. Accordingly, we observed significantly increased abnormal nuclear events, such as enlarged nuclei, misarranged chromosome alignment, failed chromosome segregation and disrupted microtubule polymerization, in MX106 treated cells (Fig. 5C-D). All these data suggest that inhibition of survivin by MX106 directly promotes cell cycle arrest and mitotic catastrophe, which may eventually leads to necrotic and apoptotic cell death in cancer cells (Vitale et al., 2011).

Survivin inhibitor sensitize TNBC tumors to chemotherapy in vivo*.*

To determine if survivin inhibitor can synergize with cytotoxic chemotherapeutic to suppress tumor growth *in vivo*, we generated an orthotopic TNBC xenograft model by injecting MDA-MB-231LM2 cells into mouse mammary fat pads as we reported previously (Niu et al., 2016). Tumor growth was monitored and tumor bearing mice were randomly separated into four treatment groups as indicated in Fig 6A. We found MX106 alone was able to reduce xenograft tumor progression. Dox treatment led to decreased tumor growth, whereas xenograft tumors soon adapted to the Dox treatment and regained the growth potential after the third injection. Combination treatment of Dox with MX106 showed significantly enhanced tumor-suppressive efficacy than treatment with either agent alone (Fig. 6A-B). Importantly, no regaining of tumor growth potential was observed after combinatory treatment until the end point, suggesting potential mitigation of acquired resistance to Dox in xenograft tumors. We also observed further decreased lung metastasis in combination treatment group, compared with single agent groups (Fig. 6C).

To validate the efficacy of MX106 in promoting degradation of survivin and other IAPs, we examined the protein lysates extracted from xenograft tumors. As expected, survivin level was significantly decreased in tumors treated with MX106 (Fig. 6D). In parallel, XIAP expression was also decreased in response to MX106 treatment while change of cIAP1 expression was negligible. Consistent with our observation *in vitro*, Dox treatment induced robust NF-κB activation in tumors, which was substantially decreased in tumors co-treated with MX106. We also observed no substantial increase of NIK level and p52 processing in tumors treated by MX106 (supplemental Fig 2B), suggesting that the alternative NF-κB signaling was not activated in these tumors. Along with decreased genotoxic NF-κB activation, we found increased PARP cleavage in tumors treated with combination of Dox with MX106, compared to those treated with Dox alone, suggesting increased tumor cell apoptosis (Fig. 6D). In addition, Dox-induced transcriptional upregulation of IL-6 and IL-8 in TNBC tumors was also significantly decreased by co-treatment with MX106, likely due to suppression of genotoxic NF-κB activation (Fig. 6E).

Discussion

Increased survivin levels have been associated with chemoresistance in a variety of malignancies (Coumar et al., 2013; Zheng, 2017). The function of survivin in regulating apoptosis, autophagy, mitosis and DNA repair are considered to play major roles in promoting cancer cell survival and evasion from tumoricidal effect of chemotherapeutics and radiation (Grdina et al., 2013). Therefore, survivin has drawn significant attention as a target of anti-cancer agents mitigating drug resistance (Xiao and Li, 2015; Peery et al., 2017). We recently developed a novel compound UC-112 with similarity to SMAC AVPI domain and its more potent derivatives MX106/MX107, which showed high efficiency in promoting survivin degradation and

inducing apoptosis in melanoma cells (Chen, 2012; Coumar et al., 2013). Here, we found that the MX106/MX107 suppressed TNBC cell growth and inhibited TNBC xenograft tumor progression *in vivo*. Although low dose of MX106/MX107 did not significantly increase apoptosis directly in cancer cells, it effectively arrested cell cycle progression and interrupted cells division, eventually leading to mitotic catastrophe. Furthermore, the survivin inhibitors synergize with genotoxic drugs or IR, and dramatically enhanced cancer cell apoptosis in response to cytotoxic treatments. We further showed that degradation of XIAP and/or cIAP1 by MX106/MX107 diminished NF-κB activation induced by these genotoxic agents, which may be responsible, at least in part, for increased drug sensitivity and apoptosis in cancer cells and TNBC xenograft tumors treated with doxorubicin. In line with this notion, survivin inhibitor YM155 failed to decrease cIAP1/XIAP expression and genotoxic NF-κB activation in TNBC cells, which may explain its lower synergism with Dox treatment in inhibiting TNBC cell proliferation compared with MX106. These results strongly suggest that the survivin inhibitors MX106/MX107 may be used in combination with chemotherapeutics, such as doxorubicin, to achieve synergistic tumoricidal effect in treating TNBC.

Anthracycline drugs, such as doxorubicin and epirubicin, are a leading cause of heart failure and irreversible cardiovascular damage in cancer patients after chemotherapy (Brown et al., 2015). The high cardiotoxicity of anthracycline drugs is a major limitation when considering chemotherapeutic regimens for cancer patients with high cardiovascular risk. We found that MX106/MX107 significantly reduced IC_{50} of doxorubicin in cancer cells, which indicates that combining MX106/MX107 with doxorubicin could substantially reduce the drug dose with comparable efficacy, resulting in reduced risk of cardiotoxicity in patients. We also observed similar effect in cancer cells treated by IR in combination of MX106, suggesting their potential application in reducing radiation dose for treating breast cancer.

Genotoxic treatment-induced NF-κB activation has been considered as a major mechanism by which cancer cells acquire drug resistance (Zheng, 2017). Our previous studies showed that, besides of anti-apoptotic genes induced by NF-κB, upregulation and secretion of inflammatory cytokines (i.e. IL-6 and IL-8) may also contribute to a chronic inflammatory microenvironment which enhances the survival and increased invasiveness in cancer cell (Niu et al., 2012; Niu et al., 2016; Wang et al., 2017). MX106/MX107 substantially reduced induction of inflammatory cytokine IL-6 and IL-8 *in vitro* and in xenograft tumors after Dox treatment. Moreover, the lung metastasis of xenograft tumors also was significantly reduced in xenografted mice treated with Dox in combination with MX106, compared to that in mice treated with Dox or MX106 alone. These data suggest that MX106/MX107-mediated suppression of NF-κB activation by chemotherapeutic drugs not only sensitizes TNBC cells to chemotherapy, but also could reduce their metastatic potential.

Previous studies have demonstrated that treatment with SMAC-memetic compounds with high potency in degrading cIAP1/2 proteins, such as BV6 and compound A, could stabilize NIK and activate alternative NF-κB signaling, thereby upregulating TNFα (Varfolomeev et al., 2007; Vince et al., 2007). Autocrine and/or paracrine of TNFα stimulate cancer cell apoptosis in the absence of cIAP1-mediated pro-survival branch of TNFα signaling, which could be further reinforced by increased complex II (RIP1/FADD/Caspase 8) formation due to decreased RIP1 ubiquitylation by cIAP1 (Fulda, 2015b). We did not observed alternative NF-κB activation and induction of apoptosis by MX106/MX107 treatment alone in breast cancer cells, it may be owing to the relative low dose we used for combination treatment. High basal p52 level in MDA-MB-231 cells may also increase the threshold for further enhancing alternative NF-κB signaling. Furthermore, MX106/MX107 and their precursor compound UC-112 have been shown to induce survivin degradation with high potency, while less effective in inducing cIAP1/2 and XIAP degradation (Xiao et al., 2015). Nevertheless, the tumoricidal effect and caspase activation in

melanoma cells by MX106/MX107 and their precursor UC-112 may involve alternative NF-κB activation and TNFα/RIP1-induced apoptotic signaling (Wang and Li, 2014; Xiao et al., 2015), which warrants further investigation.

Survivin expression is abundant in embryonic stem cells during fetal development. It also plays critical roles in homeostasis of adult stem/progenitor cells, such as hematopoietic stem cells and neuronal stem cells (Altieri, 2015). Moreover, previous reports showed that survivin overexpression initiated hematopoietic stem cell-driven malignancies in mice (Small et al., 2010), and promoted survival of glioma stem-like cells during gliomagenesis (Guvenc et al., 2013). In accordance, high survivin level is associated with poor survival in stem cell-driven tumors, such as acute leukemia and gliomas. Therefore, it is plausible that survivin has important roles in regulating cancer stem-like cell/cancer initiating cell behavior. In addition to the importance in cancer initiation and relapse, cancer stem-like cells are also a major source of drug resistant population (Oskarsson et al., 2014). Our data indicate that degradation of cIAP1/XIAP by MX106/MX107 could suppress genotoxic NF-κB activation, resulting in reduced drug resistance. Meanwhile, directly targeting survivin by MX106/MX107 may decrease cancer stem-like cell population, which could also contribute to increased drug sensitivity and mitigation of drug resistance.

In summary, we found that survivin inhibitor MX106/MX107 significantly increased therapeutic potency of doxorubicin in treating TNBC cells. Combined treatment with Dox and MX106 showed superior tumor suppressive efficacy, compared to Dox or MX106 alone, in TNBC MDA-MB-231 xenograft model. Mechanistically, MX106/MX107-induced degradation of cIAP1 and/or XIAP attenuated NF-κB activation by chemotherapeutic drugs and radiation, which sensitized cancer cells to cytotoxic treatment. Combining MX106/MX107 or other SMAC memetic compounds with anthracycline drugs may significantly improve their therapeutic efficacy, which may enable treating cancer patients with lower dose of anthracycline thereby

reducing treatment-associated cardiotoxicity. Inhibiting survivin by a variety of approaches has been shown to induce apoptosis in cancer cells (Altieri, 2015; Xiao and Li, 2015; Peery et al., 2017). Although the lower dose of MX106/MX107 did not directly induce apoptosis, it is sufficient for causing cell cycle arrest and promoting mitotic catastrophe. Moreover, the MX106/MX107 dependent inhibition of genotoxic NF-κB activation could further enhance cytotoxic treatment-induced apoptosis. Several SMAC mimetics, predominantly antagonizing cIAP1, cIAP2 and XIAP, are under evaluation in clinical trials (Fulda, 2015b; Fulda, 2015a). Meanwhile, survivin inhibitor YM155 has also been tested as a single agent or in combination with other anticancer agents for treating various solid tumors and blood cancers (Peery et al., 2017). Unlike YM155, MX106/MX107 are not sensitive to P-gp pump-mediated drug efflux (Xiao et al., 2015), indicating a reduced drug resistance prospect in cancer cells. Therefore, our novel survivin inhibitor MX106/MX107 may be able to harness the therapeutic benefit from inhibiting oncogenic activity of survivin in promoting cancer cell survival and mitosis, as well as cIAP1/XIAP-facilitated genotoxic NF-κB activation, leading to synergistic tumor-suppressive efficacy when used to in combination with genotoxic agents.

Acknowledgments.

We thank Dr. Junming Yue (UTHSC) for providing valuable reagents used in this study.

Authorship Contributions

Participated in research design: Wang, Fan, Li, Z.H. Wu

Conducted experiments: Wang, Zhang, Mani, Z. Wu, Z.H. Wu

Contributed new reagents or analytical tools: Z. Wu, Li

Performed data analysis: Wang, Fan, Z. Wu, Li, Z.H. Wu

Wrote or contributed to the writing of the manuscript: Wang, Fan, Li, Z.H. Wu

REFERENCES

Altieri DC (2015) Survivin - The inconvenient IAP. *Seminars in cell & developmental biology* **39**:91-96.

Baldwin AS (2012) Regulation of cell death and autophagy by IKK and NF-kappaB: critical mechanisms in immune function and cancer. *Immunol Rev* **246**:327-345.

Bianchini G, Balko JM, Mayer IA, Sanders ME and Gianni L (2016) Triple-negative breast cancer: challenges and opportunities of a heterogeneous disease. *Nat Rev Clin Oncol* **13**:674-690.

Brown SA, Sandhu N and Herrmann J (2015) Systems biology approaches to adverse drug effects: the example of cardio-oncology. *Nat Rev Clin Oncol* **12**:718-731.

Carmena M, Wheelock M, Funabiki H and Earnshaw WC (2012) The chromosomal passenger complex (CPC): from easy rider to the godfather of mitosis. *Nat Rev Mol Cell Biol* **13**:789-803.

Chen ZJ (2012) Ubiquitination in signaling to and activation of IKK. *Immunol Rev* **246**:95-106.

Chou TC (2010) Drug combination studies and their synergy quantification using the Chou-Talalay method. *Cancer Res* **70**:440-446.

Coumar MS, Tsai FY, Kanwar JR, Sarvagalla S and Cheung CH (2013) Treat cancers by targeting survivin: just a dream or future reality? *Cancer treatment reviews* **39**:802-811.

Foulkes WD, Smith IE and Reis-Filho JS (2010) Triple-Negative Breast Cancer. *N Engl J Med* **363**:1938-1948.

Fu K, Sun X, Wier EM, Hodgson A, Liu Y, Sears CL and Wan F (2016) Sam68/KHDRBS1 is critical for colon tumorigenesis by regulating genotoxic stress-induced NF-kappaB activation. *eLife* **5**.

Fulda S (2015a) Promises and Challenges of Smac Mimetics as Cancer Therapeutics. *Clin Cancer Res* **21**:5030-5036.

Fulda S (2015b) Smac mimetics as IAP antagonists. *Seminars in cell & developmental biology* **39**:132-138.

Garg H, Suri P, Gupta JC, Talwar GP and Dubey S (2016) Survivin: a unique target for tumor therapy. *Cancer cell international* **16**:49.

Grdina DJ, Murley JS, Miller RC, Mauceri HJ, Sutton HG, Li JJ, Woloschak GE and Weichselbaum RR (2013) A Survivin-Associated Adaptive Response in Radiation Therapy. *Cancer Res* **73**:4418-4428.

Guvenc H, Pavlyukov MS, Joshi K, Kurt H, Banasavadi-Siddegowda YK, Mao P, Hong C, Yamada R, Kwon CH, Bhasin D, Chettiar S, Kitange G, Park IH, Sarkaria JN, Li C, Shakhparonov MI and Nakano I (2013) Impairment of glioma stem cell survival and growth by a novel inhibitor for Survivin-Ran protein complex. *Clin Cancer Res* **19**:631-642.

Hinz M, Stilmann M, Arslan Sc, Khanna KK, Dittmar G and Scheidereit C (2010) A Cytoplasmic ATM-TRAF6-cIAP1 Module Links Nuclear DNA Damage Signaling to Ubiquitin-Mediated NF-kappaB Activation. *Mol Cell* **40**:63-74.

Holohan C, Van Schaeybroeck S, Longley DB and Johnston PG (2013) Cancer drug resistance: an evolving paradigm. *Nat Rev Cancer* **13**:714-726.

Huang TT, Wuerzberger-Davis SM, Wu ZH and Miyamoto S (2003) Sequential modification of NEMO/IKKgamma by SUMO-1 and ubiquitin mediates NF-kappaB activation by genotoxic stress. *Cell* **115**:565-576.

Jin H-S, Lee D-H, Kim D-H, Chung J-H, Lee S-J and Lee TH (2009) cIAP1, cIAP2, and XIAP Act Cooperatively via Nonredundant Pathways to Regulate Genotoxic Stress-Induced Nuclear Factor-{kappa}B Activation. *Cancer Res* **69**:1782-1791.

Kedinger V, Meulle A, Zounib O, Bonnet ME, Gossart JB, Benoit E, Messmer M, Shankaranarayanan P, Behr JP, Erbacher P and Bolcato-Bellemin AL (2013) Sticky

siRNAs targeting survivin and cyclin B1 exert an antitumoral effect on melanoma subcutaneous xenografts and lung metastases. *BMC Cancer* **13**:338.

Lanczky A, Nagy A, Bottai G, Munkacsy G, Szabo A, Santarpia L and Gyorffy B (2016) miRpower: a web-tool to validate survival-associated miRNAs utilizing expression data from 2178 breast cancer patients. *Breast Cancer Res Treat* **160**:439-446.

Li S, Wang L, Meng Y, Chang Y, Xu J and Zhang Q (2017) Increased levels of LAPTM4B, VEGF and survivin are correlated with tumor progression and poor prognosis in breast cancer patients. *Oncotarget* **8**:41282-41293.

Mabb AM, Wuerzberger-Davis SM and Miyamoto S (2006) PIASy mediates NEMO sumoylation and NF-kappaB activation in response to genotoxic stress. *Nat Cell Biol* **8**:986-993.

McCool KW and Miyamoto S (2012) DNA damage-dependent NF-kappaB activation: NEMO turns nuclear signaling inside out. *Immunol Rev* **246**:311-326.

Mitra A, Mishra L and Li S (2015) EMT, CTCs and CSCs in tumor relapse and drug-resistance. *Oncotarget* **6**:10697-10711.

Nakanishi C and Toi M (2005) Nuclear factor-kappaB inhibitors as sensitizers to anticancer drugs. *Nat Rev Cancer* **5**:297-309.

Niu J, Shi Y, Tan G, Yang CH, Fan M, Pfeffer LM and Wu ZH (2012) DNA damage induces NF-kappaB-dependent microRNA-21 upregulation and promotes breast cancer cell invasion. *J Biol Chem* **287**:21783-21795.

Niu J, Shi Y, Xue J, Miao R, Huang S, Wang T, Wu J, Fu M and Wu ZH (2013) USP10 inhibits genotoxic NF-kappaB activation by MCPIP1-facilitated deubiquitination of NEMO. *EMBO J* **32**:3206-3219.

Niu J, Xue A, Chi Y, Xue J, Wang W, Zhao Z, Fan M, Yang CH, Shao ZM, Pfeffer LM, Wu J and Wu ZH (2016) Induction of miRNA-181a by genotoxic treatments promotes chemotherapeutic resistance and metastasis in breast cancer. *Oncogene* **35**:1302-1313.

Oskarsson T, Batlle E and Massague J (2014) Metastatic stem cells: sources, niches, and vital pathways. *Cell Stem Cell* **14**:306-321.

Peery RC, Liu JY and Zhang JT (2017) Targeting survivin for therapeutic discovery: past, present, and future promises. *Drug discovery today* **22**:1466-1477.

Pennati M, Binda M, Colella G, Zoppe M, Folini M, Vignati S, Valentini A, Citti L, De Cesare M, Pratesi G, Giacca M, Daidone MG and Zaffaroni N (2004) Ribozyme-mediated inhibition of survivin expression increases spontaneous and drug-induced apoptosis and decreases the tumorigenic potential of human prostate cancer cells. *Oncogene* **23**:386-394.

Ryan B, O'Donovan N, Browne B, O'Shea C, Crown J, Hill AD, McDermott E, O'Higgins N and Duffy MJ (2005) Expression of survivin and its splice variants survivin-2B and survivin-DeltaEx3 in breast cancer. *Br J Cancer* **92**:120-124.

Singh A and Settleman J (2010) EMT, cancer stem cells and drug resistance: an emerging axis of evil in the war on cancer. *Oncogene* **29**:4741-4751.

Small S, Keerthivasan G, Huang Z, Gurbuxani S and Crispino JD (2010) Overexpression of survivin initiates hematologic malignancies in vivo. *Leukemia* **24**:1920-1926.

Stilmann M, Hinz M, Arslan SC, Zimmer A, Schreiber V and Scheidereit C (2009) A Nuclear Poly(ADP-Ribose)-Dependent Signalosome Confers DNA Damage-Induced IkB Kinase Activation. *Mol Cell* **36**:365-378.

Varfolomeev E, Blankenship JW, Wayson SM, Fedorova AV, Kayagaki N, Garg P, Zobel K, Dynek JN, Elliott LO, Wallweber HJA, Flygare JA, Fairbrother WJ, Deshayes K, Dixit VM and Vucic D (2007) IAP Antagonists Induce Autoubiquitination of c-IAPs, NF-κB Activation, and TNFα-Dependent Apoptosis. *Cell* **131**:669-681.

Vince JE, Wong WW-L, Khan N, Feltham R, Chau D, Ahmed AU, Benetatos CA, Chunduru SK, Condon SM, McKinlay M, Brink R, Leverkus M, Tergaonkar V, Schneider P, Callus BA,

Koentgen F, Vaux DL and Silke J (2007) IAP Antagonists Target cIAP1 to Induce TNFα-Dependent Apoptosis. *Cell* **131**:682-693.

Vitale I, Galluzzi L, Castedo M and Kroemer G (2011) Mitotic catastrophe: a mechanism for avoiding genomic instability. *Nat Rev Mol Cell Biol* **12**:385-392.

Wang J and Li W (2014) Discovery of novel second mitochondria-derived activator of caspase mimetics as selective inhibitor of apoptosis protein inhibitors. *The Journal of pharmacology and experimental therapeutics* **349**:319-329.

Wang W, Mani AM and Wu ZH (2017) DNA damage-induced nuclear factor-kappa B activation and its roles in cancer progression. *J Cancer Metastasis Treat* **3**:45-59.

Wu ZH and Miyamoto S (2007) Many faces of NF-kappaB signaling induced by genotoxic stress. *J Mol Med* **85**:1187-1202.

Wu ZH, Shi Y, Tibbetts RS and Miyamoto S (2006) Molecular linkage between the kinase ATM and NF-kappaB signaling in response to genotoxic stimuli. *Science* **311**:1141-1146.

Wu ZH, Wong ET, Shi Y, Niu J, Chen Z, Miyamoto S and Tergaonkar V (2010) ATM- and NEMO-dependent ELKS ubiquitination coordinates TAK1-mediated IKK activation in response to genotoxic stress. *Mol Cell* **40**:75-86.

Xiao M and Li W (2015) Recent Advances on Small-Molecule Survivin Inhibitors. *Current medicinal chemistry* **22**:1136 - 1146.

Xiao M, Wang J, Lin Z, Lu Y, Li Z, White SW, Miller DD and Li W (2015) Design, Synthesis and Structure-Activity Relationship Studies of Novel Survivin Inhibitors with Potent Anti-Proliferative Properties. *PLoS ONE* **10**:e0129807.

Zheng HC (2017) The molecular mechanisms of chemoresistance in cancers. *Oncotarget* **8**:59950-59964.

Footnotes

This work was supported in part by grants from the National Cancer Institute (R01 CA149251 to Z.W. and R01CA193609 to W.L.), National Natural Science Foundation of China (81528016), American Cancer Society (RSG-13-186-01-CSM), and Jiangsu Provincial Key R&D Special Fund (BE2015666).

JPET Fast Forward. Published on May 7, 2018 as DOI: 10.1124/jpet.118.249151
This article has not been copyedited and formatted. The final version may differ from this version.

FIGURE LEGENDS

Figure 1: Survivin inhibitor MX106 and MX107 synergize with genotoxic treatments in suppressing tumor cell growth.

(A) High survivin levels associated with poor prognosis in breast cancer patients. Data were retrieved from KMplot.com. Left, Kaplan-Meier analyses of overall survival (OS) in breast cancer patients stratified by *BIRC5* levels. Right, Kaplan-Meier analyses of recurrence-free survival (RFS) in TNBC patients based on *BIRC5* levels. **(B)** MDA-MB-231 cells were treated with varying doses of MX106 or MX107 for 24 hours. Cell viability was determined by CCK-8 assay. The IC_{50} of MX106 and MX107 was 2.2 μM and 3.1 μM respectively. **(C)** MDA-MB-231 cells were treated by Dox alone or in combination with MX106 for 24 hours. Cell viability was analyzed as in B. **(D)** CI values of combination treatment of MX106 and Dox in MDA-MB-231 cells were calculated and plotted using CompuSyn. **(E)** Combination effect of MX106 with Dox in U2OS cells was analyzed as in C. The IC_{50} of Dox alone is 3.4 ng/ml, and decreased to 0.6 ng/ml when combining MX106 treatment. **(F)** MDA-MB-231 cells were treated with IR alone or in combination of pretreatment of MX106 (1 μM) for 12 h. Cell viability was determined at 48 h after radiation.

Figure 2: MX106/MX107 significantly enhance genotoxic drug-induced apoptosis.

(A) MDA-MB-231 cells were treated with Dox (2 μg/ml), MX106 (3 μM) or in combination. Crystal violet staining was used to determine cell survival at 2 days after treatment. **(B)** MDA-MB-231 cells were treated by Dox (0.5 μg/ml) and/or MX106 (2 μM) and analyzed by flow cytometry after Annexin V-FITC/PI staining. **(C)** and **(D)**. HEK293 (C) and MDA-MB-231 (D) cells were treated with Etoposide (VP16, 10 μM) or Dox (2 μg/ml) alone or in combination with MX106 (3 μM) or MX107 (3 μM). Then, cells were harvested for immunoblotting with indicated antibodies.

Figure 3: MX106/MX107 inhibit NF-κB activation by genotoxic agents.

(A) MDA-MB-231 pretreated by DMSO or increasing doses of MX106 for 12 h were exposed to Dox (2 μg/ml) for 2 h as indicated. NF-κB activity was examined by EMSA. Whole cell extracts were analyzed by western blotting with indicated antibodies. **(B)** HEK293 cells were pretreated with DMSO, MX106 (3 μM) or MX107 (3 μM) for 12 h. Cells were then exposed to IR (10 Gy) and harvest at 2 h after treatment. Whole cell extracts were analyzed as in A. **(C)** U2OS cells were treated by Dox (2 μg/ml) with or without MX106/MX107 pretreatment as in B and analyzed by immunoblotting as indicated. **(D)** HEK293 cells were treated with TNFα (10 ng/ml, 15 min) or VP16 (10 μM, 2h) in a setting similar to B. whole cell lysates were analyzed accordingly. **(E)** The transactivity of NF-κB was monitored with NF-κB Luciferase reporter in MDA-MB-231 cells after indicated treatment. **(F)** The mRNA levels of IL-6, IL-8 and IκBα (NFKBIA) were analyzed by qPCR in MDA-MB-231 cells treated by Dox (2 μg/ml), MX106 (3 μM), MX107 (3 μM) alone or in combination as indicated.

Figure 4: MX106/MX107 suppress DNA damage-induced activation of TAK1/IKK by promoting cIAP1/XIAP degradation.

(A) HEK293T cells were pretreated with DMSO, MX106 (3 μM) or MX107 (3 μM) for 12 h. Cells were then exposed to VP16 (10 μM) and harvest at 1 h after treatment. Whole cell extracts were immunoprecipitated with anti-NEMO, followed by immunoblotting with antibodies as shown. 5% of whole cell extracts were used as input control. **(B)** HEK293T cells were treated as in A. ELKS were immunoprecipitated by respective antibodies. Immunoprecipitates were blotted by K63 ub linkage-specific antibody as indicated. 5% of whole cell lysates as input were analyzed by western blot as shown. **(C)** HEK293T cells were treated as in B. TAK1 kinase activity were determined by *in vitro* kinase assay using GST-IKKβ as substrate. Whole cell extracts were analyzed by immunoblotting as indicated. **(D)** IKK activity in cells treated as in C were measured by kinase assay using GST-IκBα as substrate.

JPET Fast Forward. Published on May 7, 2018 as DOI: 10.1124/jpet.118.249151
This article has not been copyedited and formatted. The final version may differ from this version.

Figure 5: Antagonizing survivin by MX106 leads to cell cycle arrest and abnormal cell division.

(A) Survivin was depleted by siRNA in HEK293T cells. NF-κB activation upon VP16 treatment (10 μM, 2h) was examined by EMSA as indicated. **(B)** Cell cycle in control or MX106 treated (3 μM, 48 h) MDA-MB-231 cells was examined by flow cytometry. **(C)** and **(D)**. Mitotic cells and cell division were visualized by immunofluorescence staining with anti-αTubulin and DAPI in control or MX106-treated (2 μM, 48 h) MDA-MB-231 cells. Representative abnormal microtubule spindles and aberrant cell division upon MX106 treatment were shown in (C), and were quantified as abnormal nuclear events in (D).

Figure 6: Survivin inhibitor MX106 shows synergism with Dox treatment in suppressing tumor growth and metastasis *in vivo*.

(A) NSG mice transplanted with MDA-MB-231 LM2 cells (n=5) were treated with PBS, Dox (2 mg/kg), MX106 (20mg/kg) or in combination when xenograft tumor volume reached ~100 mm^3 as shown. Xenograft tumor growth was monitored and showed as the tumor volume. Red arrow: Dox or N.S. treatment; purple arrow: MX106 injection. *: $p< 0.05$. **(B)** Bioluminescence imaging was performed at the experiment end point to visualize tumor size. **(C)** Pulmonary tumor outgrowth was monitored by bioluminescent imaging as in B. **(D)** Protein samples extracted from xenograft tumors (2/group) were immunoblotted by antibodies against p-P65, p65, cleaved PARP, XIAP, survivin, and tubulin. **(E)** RNA samples were extracted from tumors and analyzed by qPCR.

JPET Fast Forward. Published on May 7, 2018 as DOI: 10.1124/jpet.118.249151
This article has not been copyedited and formatted. The final version may differ from this version.

Figure 1

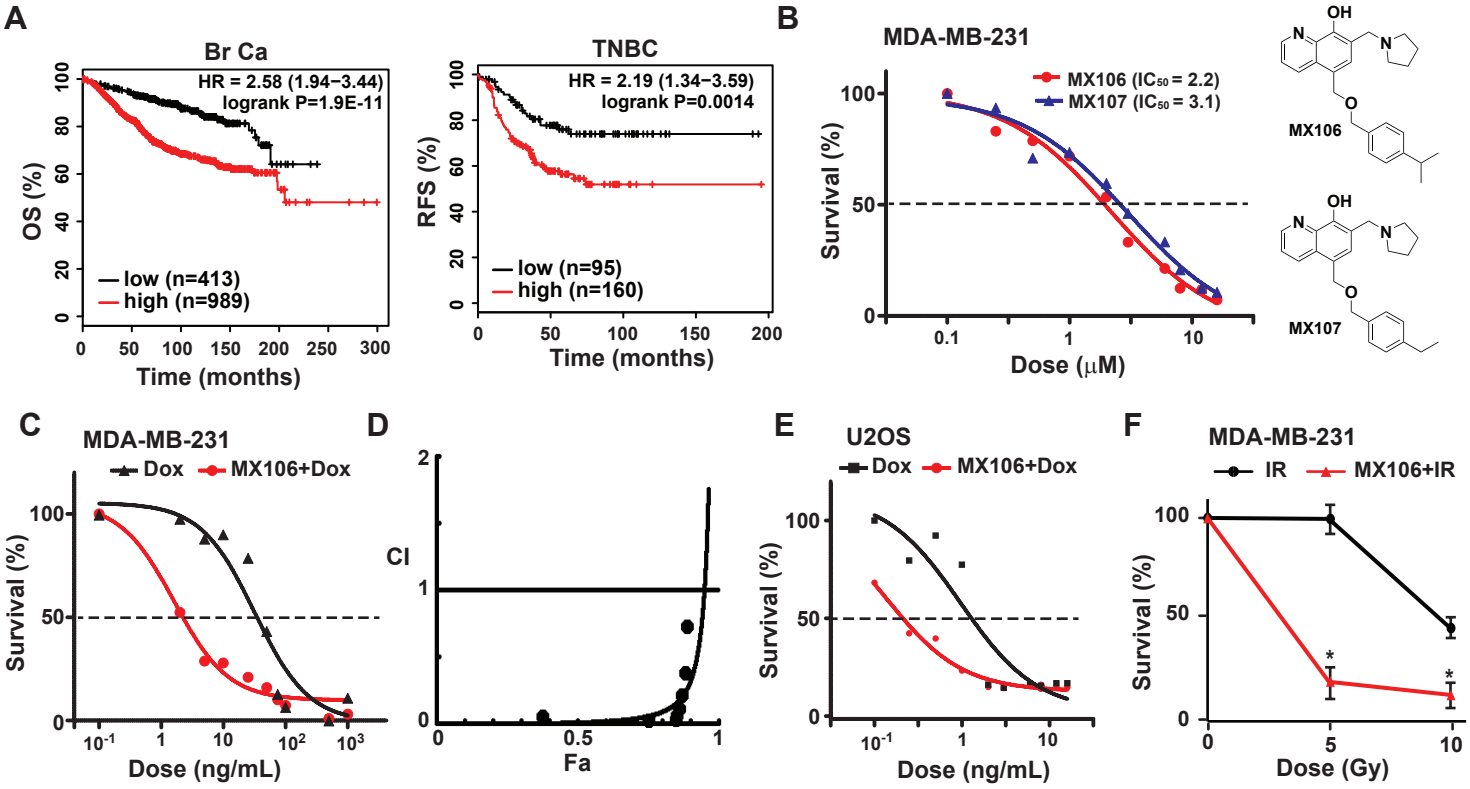

JPET Fast Forward. Published on May 7, 2018 as DOI: 10.1124/jpet.118.249151
This article has not been copyedited and formatted. The final version may differ from this version.

Figure 2

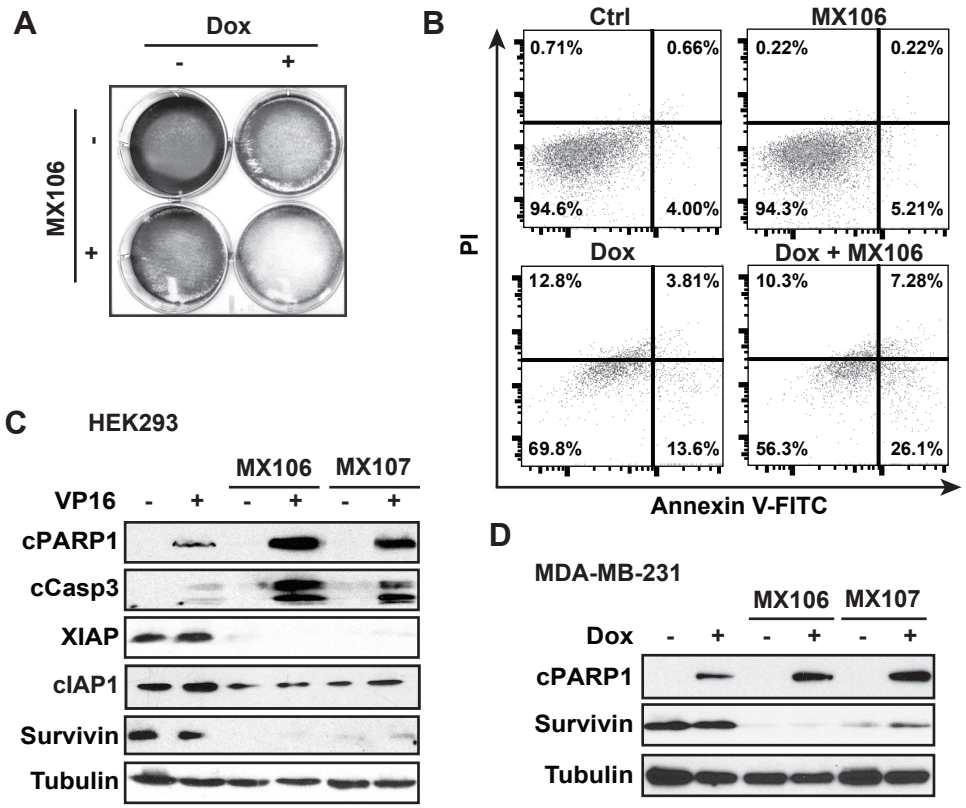

JPET Fast Forward. Published on May 7, 2018 as DOI: 10.1124/jpet.118.249151
This article has not been copyedited and formatted. The final version may differ from this version.

Figure 3

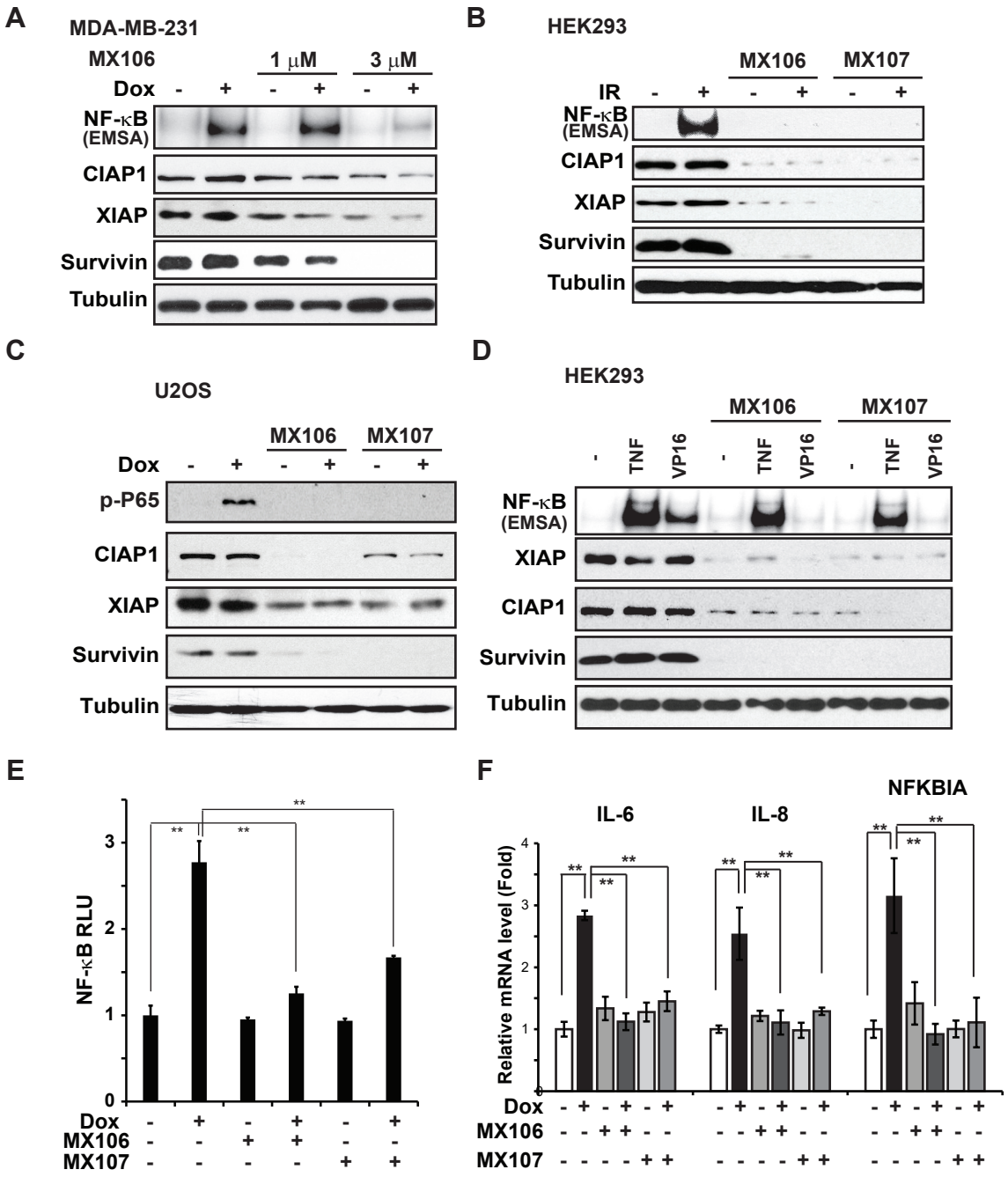

JPET Fast Forward. Published on May 7, 2018 as DOI: 10.1124/jpet.118.249151
This article has not been copyedited and formatted. The final version may differ from this version.

Figure 4

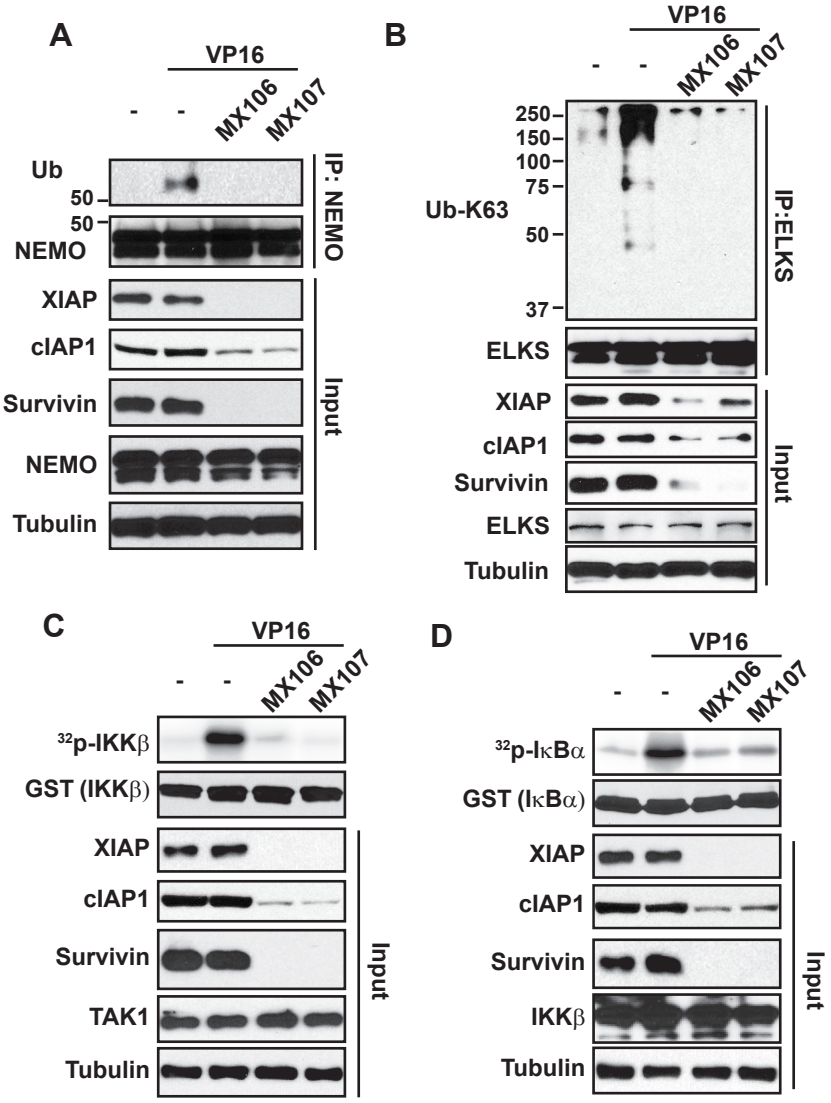

Figure 5

JPET Fast Forward. Published on May 7, 2018 as DOI: 10.1124/jpet.118.249151
This article has not been copyedited and formatted. The final version may differ from this version.

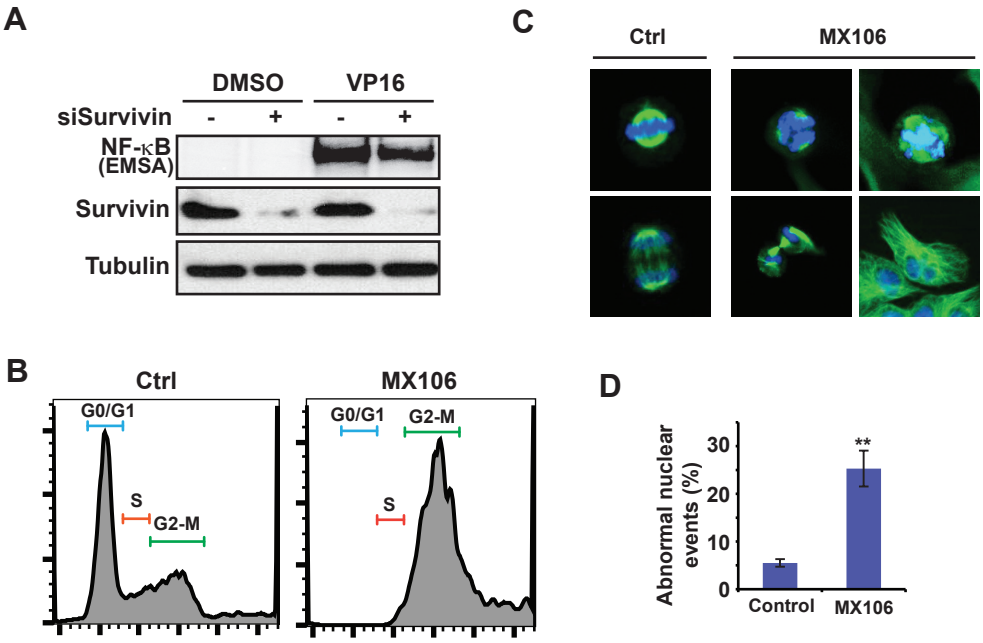

Figure 6

JPET Fast Forward. Published on May 7, 2018 as DOI: 10.1124/jpet.118.249151
This article has not been copyedited and formatted. The final version may differ from this version.